Pergamon

Int. J. Solids Structures Vol. 32, No. 6/7, pp. 939–955, 1995

0020–7683/95 $9.50 + .00

0020–7683(94)00170–7

AN INTERPRETATION OF TWYMAN–GREEN INTERFEROGRAMS FROM STATIC AND DYNAMIC FRACTURE EXPERIMENTS

R. D. PFAFF,† P. D. WASHABAUGH,‡ and W. G. KNAUSS
Graduate Aeronautics Laboratories, California Institute of Technology, Pasadena, California, U.S.A.

(*Received* 1 *February* 1994; *in revised form*, 29 *April* 1994)

Abstract—The application of a Twyman–Green interferometer to measurements in static and dynamic fracture mechanics is described. Twyman–Green interferometry shows the absence of a dominant singular field in the out-of-plane deformation in the vicinity of a crack. For relatively brittle fracture and except near the crack flanks, the spatial gradient of the out-of-plane displacement for a quasi-statically propagating crack is well predicted by elastostatic simulations. In addition, this method has been employed to elucidate certain transient features involving cracks propagating at large fractions of the material wave speeds. The free surface out-of-plane deformation surrounding a constant velocity dynamically propagating crack in a plate is compared with the equivalent elastostatic case. It appears that the dynamic deformation may not be obtained from the static deformation simply by a Prandtl–Glauert mapping as might be suggested by the solution for the equivalent two-dimensional generalized plane stress problem. Alternatively, the general character of the three-dimensional dynamic surface deformation may be approximately fitted by a Doppler mapping of the static deformation when scaled by the crack to plate wave speed ratio.

1. INTRODUCTION

In the early stages of an experimental endeavor, a researcher invariably must choose between employing an existing measurement technique or developing an entirely new approach. For any given epoch this selection is typically severely constrained by available resources. The development of a new method is fraught with additional burdens and hazards that have been remedied for an established approach. With a new technique not only must the original measurement task be performed, but the design, construction, and adjustment of the method itself must also be explored. Further, a new method runs the risk of utterly failing, or at least not meeting expectations due to some unforeseen hurdle.

Even with such additional obstacles and risks, the impetus to develop new methods, or at least improve an existing observation, stems from several sources. Typically, after an experiment has been performed, the experience leads to straightforward improvements in the technique. However, more significantly, after a whole set of observations have been made with an established (and perhaps incrementally improved) method, fundamental questions frequently remain. Many times these fundamental issues deal with aspects of the experiment that were not measured, hence serving as an incentive to refine and expand the observations. For instance, one aspect of the debate concerning the existence of a unique velocity versus stress intensity relationship for any given material stems in a large part from the experimental methods employed. When a technique that averages properties through the thickness is used such a relationship appears to exist (Irwin *et al.*, 1979). However, the results from a spatially more precise experiment (Knauss and Ravi-Chandar, 1985) do not support this conclusion. Part of the uncertainty here is that the details of the crack advance are often not measured with sufficient temporal or spatial resolution.

Thus, partially due to practical concerns and the interplay with theory, experiments such as those performed in fracture mechanics have tended to evolve slowly from studies on global properties of failure to investigations that are refined to observe local behavior. For instance, early studies established the global energetics of quasi-static brittle failure

† Now at Ariadne Engineering, Poughkeepsi, New York, U.S.A.
‡ Now at Department of Aerospace Engineering, University of Michigan, Ann Arbor, Michigan, U.S.A.

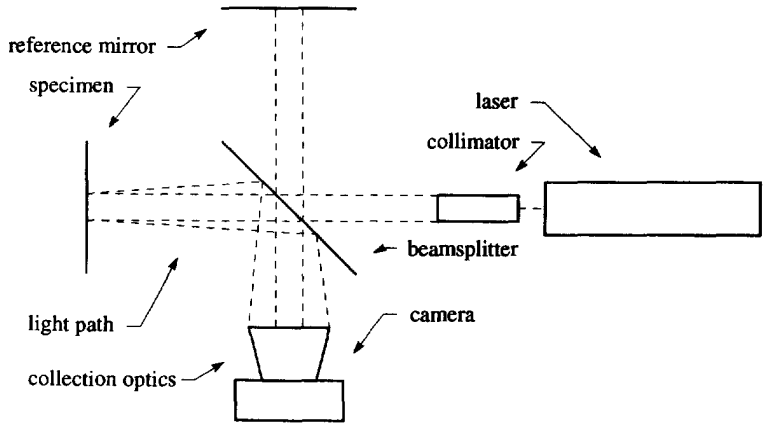

Fig. 1. Schematic of the Twyman–Green interferometer to measure out-of-plane displacement (Pfaff, 1991).

(Griffith, 1920) and later investigations settled issues dealing with the through-the-thickness average field properties surrounding a slowly moving crack [see for example Wells and Post (1954); Bradley and Kobayashi (1970)]. Other studies have led to improved spatial and temporal resolution [see for example Theocaris (1963); Kim (1985)], as well as to the measurement of aspects of the entire field surrounding a crack [see for example Dudderar and O'Regan (1971); Smith (1973)]. Recent efforts have sought to maximize aspects of the spatial and temporal resolution, simultaneously with making the measurement technique directly interpretable in terms of fracture mechanics quantities (Rosakis and Zehnder, 1985) by either automation (Sutton *et al.*, 1992) or by special diagnostics during the experiment (Tippur *et al.*, 1991).

Twyman–Green interferometry, as applied to dynamic fracture, is another step toward improving a fracture mechanicians' observational skills. However, rather than attempt to make results directly interpretable in terms of known theoretical results, the emphasis here is to develop a technique that unambiguously measures properties of the fractures process at small spatial and temporal resolutions. The motivation for introducing this particular technique by discussing and comparing prior measurement methods [for example Creath (1989)], and its development and tailoring to dynamic fracture, is left for a separate report (Pfaff *et al.*, 1994). Instead, evidence that the method has significant merit is provided by way of example experiments discussed in the following section. The remaining sections interpret these measurements. Section 3 summarizes, by way of a mathematical function, a theoretical perfectly elastic out-of-plane displacement field. This field is compared to the measurements and found to agree remarkably well except near the crack flanks where some plastic wake is to be expected. Since theoretical (analytical or numerical) results for the out-of-plane displacement field are generally unavailable, Section 4 interprets the dynamic crack measurement in terms of similarity rules. A Doppler similarity transformation of the static out-of-plane displacement is found to predict certain features of the dynamic measurements provided the dominant material wave speed is taken as the three-dimensional dilatational wave speed. The final section summarizes some implications of these results.

2. RECENT OBSERVATIONS

The interferometer shown in Fig. 1 has been used in several recent experiments concerning propagation of a crack in thin sheets of polymethylmethacrylate (PMMA). It operates by interfering the light between a reference and specimen surface. Thus, if the reference surface is flat (as shown here), the interference pattern describes the deviation of the specimen surface from planarity. In more detail, the instrument functions by splitting a coherent plane wave of light at a beam splitter. The two plane waves reflect off two separate surfaces and are then recombined and interfere at the same beam splitter. The light is then collected and recorded by a camera of sufficient capability (Pfaff, 1991).

The sheets used in the experiments described below were nominally 30 cm square by 4.7 mm thick, were loaded under quasi-static and dynamic loading conditions. The quasi-static loading was applied far above and below the crack flanks in a "single edge notch" configuration (Washabaugh, 1990). The dynamic loading was accomplished by an electromagnetic loading strip along the crack flanks several plate thicknesses from the crack tip (Washabaugh and Knauss, 1993). In addition, by a slight perturbation in the local strength properties along a very thin region (~ 10 μm), the crack could be made to propagate at velocities approaching the Rayleigh wave speed of the material (Washabaugh and Knauss, 1994).

These present experiments provide information on the out-of-plane displacement contours of the surface in the vicinity of a crack moving at velocities ranging from 10^{-6} mm/μs to near 1 mm/μs. Interferograms for this velocity range are shown below in Figs 2–4.

Figure 2 shows the out-of-plane displacement contours near the tip of a slowly propagating crack. Since the original specimen in the region of this figure was already flat to within a fringe, the only processing done to this photograph was to adjust the contrast. The white region along the crack flanks (abscissa values less than -2 mm) is a surface notch that does not extend through the thickness and was left over from the crack initiation procedure. Also present in the lower right hand corner is a circular feature caused by a small defect on the surface. A notable quality of the original of this photograph is that the data extends to within a micrometer of the crack tip (Pfaff, 1991).

Figures 3 and 4 show the contours surrounding cracks moving at an appreciable fraction of the Rayleigh wave speed. Both specimens were impulsively loaded along the crack flanks (far outside the field displayed) by an electromagnetic loading coil. The data was taken before waves could propagate to the edges of the material and back to the crack, thus simulating (for a brief instant) an infinite plate. The white regions in the photographs are attributed to angular aperture limitations of the collection optics. Both of these figures required extensive processing of the original data to remove the initially non-flat surface shape (Washabaugh and Knauss, 1994). The main difference between the two configurations is that the data shown in Fig. 3 is from an unperturbed or virgin specimen. The specimen that provided Fig. 4 had a small, almost imperceptible defect or interface, co-aligned with the propagating crack. This co-aligned defect had the effect of robbing the local material system of strength, with one consequence being an increase in the crack propagation velocity (Washabaugh and Knauss, 1994). Figure 3 provides direct evidence of a crack that is unsteadily propagating with a specific period (Washabaugh and Knauss, 1993).

3. THEORETICAL STATIC OUT-OF-PLANE DISPLACEMENT

In recent years numerous numerical investigations have been performed in an effort to understand the three-dimensional elastodynamic field in the vicinity of a crack [see for example Burton *et al.* (1984); Nakamura and Parks (1988); Parsons *et al.* (1986); Smith and Freund (1988); Krishnaswamy *et al.* (1991)]. With the existence of these studies, it is natural to compare these theoretical predictions with the Twyman–Green interferograms presented here. Due to several, perhaps unavoidable, constraints, such as publication limits, many of the studies only explicitly report aspects of their work that are deemed of interest in that particular publication. The unadulterated out-of-plane displacement field is rarely in this category. Instead the out-of-plane displacement is usually filtered through some experimental technique such as caustics (Smith and Freund, 1988). In addition, frequently the configuration of the specimen in the numerical simulation differs from that found in the experiment, thus leading an experimentalist to reproduce the numerical work for each particular experiment.

Fortunately, Nakamura and Parks (1988) addressed a problem numerically that has certain intrinsic features for any properly scaled experiment. Specifically, he investigated the three-dimensionality of the displacement field of a planar structure loaded at several plate thicknesses from the crack by the singular term or "K-field" of a planar approximation to the equations of elastostatics (Taudou *et al.*, 1992). Notably several graphs were available

describing the three-dimensional deformation near the tip of the crack.† For more general fully three-dimensional cases, the three-dimensional corrections to generalized plane stress are much less dramatic for each of the higher order terms in the generalized crack field than the correction to the plane stress "*K*-field" term. Therefore, the plane stress form will often suffice when superimposing these higher order terms with Nakamura's fully three-dimensional "*K*-field" to form solutions for those cases of more general far-field loading conditions. It is important not to forget however, that the residual parabolic through thickness boundary tractions associated with the $r^{1/2}f_1(\theta)$ and $r^{3/2}f_3(\theta)$ terms in the generalized plane stress series are also singular.

Shown in eqn (1) is a normalized function $\hat{u}_3$, that can be used to fit Nakamura's out-of-plane displacement field. The form of this equation is motivated by noting that self equilibrating fields in elastostatics have an exponential decay (Sokolnikoff, 1956) and that care was taken to insure a smooth transition to the out-of-plane displacement field from the plane stress approximation. Equation (2) defines a normalized radius, and eqn (3) is used to convert between polar and Cartesian coordinates. Equation (1) can be fitted to Nakamura's out-of-plane displacement field to within approximately 0.5% using the parameters defined in eqn (4) (Pfaff *et al.*, 1994):

$$\hat{u}_3(r_n,\theta) = \frac{1}{r_n}\left[1-e^{-a_1 r_n\left(1+\frac{1}{5}r_n^2\right)}\right]\cdot\left[1-a_2\,e^{-a_3 r_n(1+3r_n)}\right]\left[1+\frac{1}{54}e^{-\frac{1}{2}\left(r_n^2-\frac{6}{5}\pi\right)^2}\right]$$
$$\cdot\left[\cos\left(\frac{\theta}{2}\right)+a_4\left(\frac{\theta}{\pi}\right)^2 e^{-a_5 r_n(1+a_6 r_n)}-\frac{6}{31}\left(\frac{\theta}{\pi}\right)^2\left(\left(\frac{\theta}{\pi}\right)^2-\left(\frac{7}{9}\right)^2\right)\left(2e^{-2r_n}-e^{\frac{-1}{12}r_n^5}\right)\right] \quad (1)$$

$$r_n = \sqrt{2\pi\frac{r}{t}} \quad (2)$$

$$x_1 = \cos(\theta)\,r, \quad x_2 = \sin(\theta)\,r \quad (3)$$

$$a_1 = 1.07473$$
$$a_2 = 0.130624$$
$$a_3 = 3.025$$
$$a_4 = 1.05335$$
$$a_5 = 0.7258$$
$$a_6 = 0.7172. \quad (4)$$

A contour plot of eqn (1) using these parameters is shown in Fig. 5.

Confidence that eqn (1), with the parameters specified as in eqn (4), is indeed a repeatable result can be obtained by comparing aspects of the function to other three-dimensional studies. In particular the contour shapes match the out-of-plane displacement presented by Krishnaswamy *et al.* (1991) to within a contour. This study investigated the three-dimensional nature of a dynamically loaded three point bend specimen with a stationary crack. Although it would seem incongruous to compare an elastostatic solution to an elastodynamic solution, the data presented by Krishnaswamy *et al.* (1991) is for a sufficiently long time after the initiation of loading that the deformation within a plate thickness of the crack tip should be tending toward its elastostatic form. The field surrounding the crack in the three point bend specimen, unlike the study by Nakamura, contains at least the next higher order term in the plane stress approximation (Williams, 1957). The coefficient for this term can be obtained directly from Krishnaswamy's paper at non-dimensional radial distances greater than 1 and along the axis of symmetry in front of the crack. Thus a new

† The authors gratefully acknowledge Professor Nakamura for supplying the raw numerical data for his out-of-plane displacement figures, thus contributing to the accuracy of the fit.

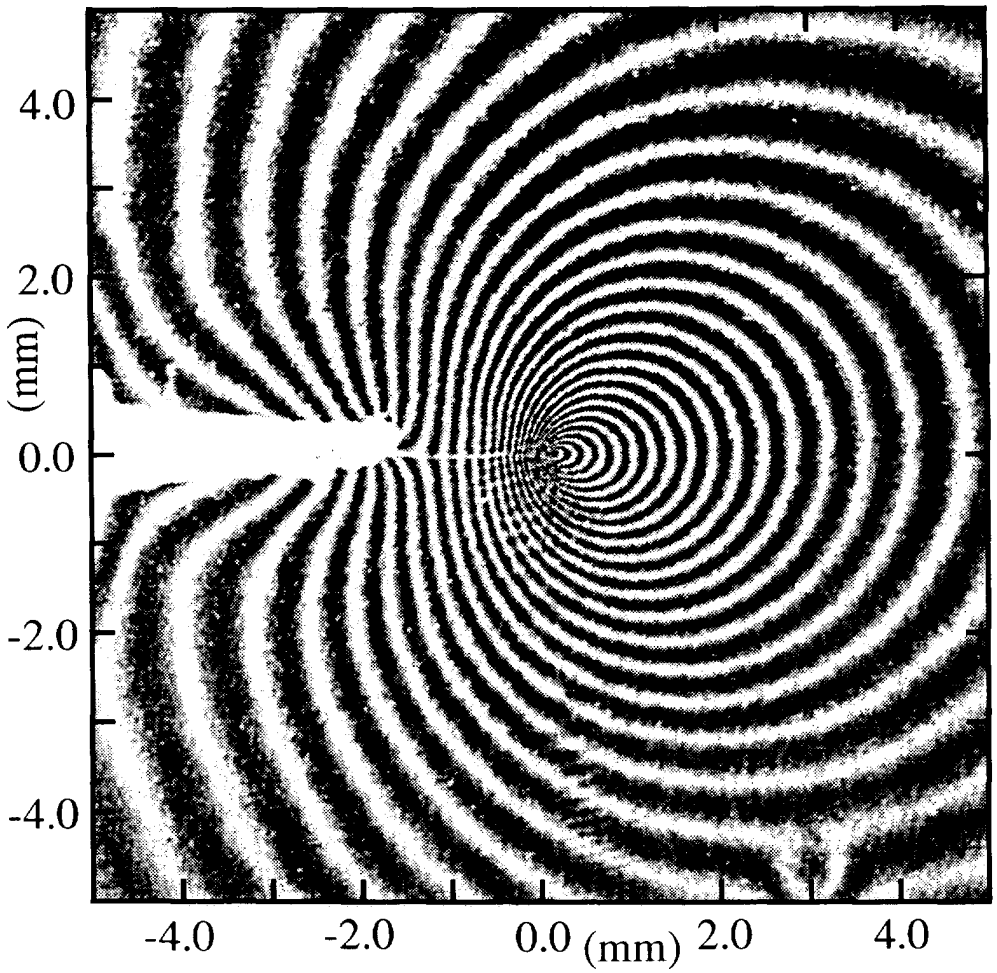

Fig. 2. An interferogram of the out-of-plane surface displacement of a quasi-statically moving crack 4.66 mm thick plate of polymethylmethacrylate. Contours represent a 312 nm change in elevation.

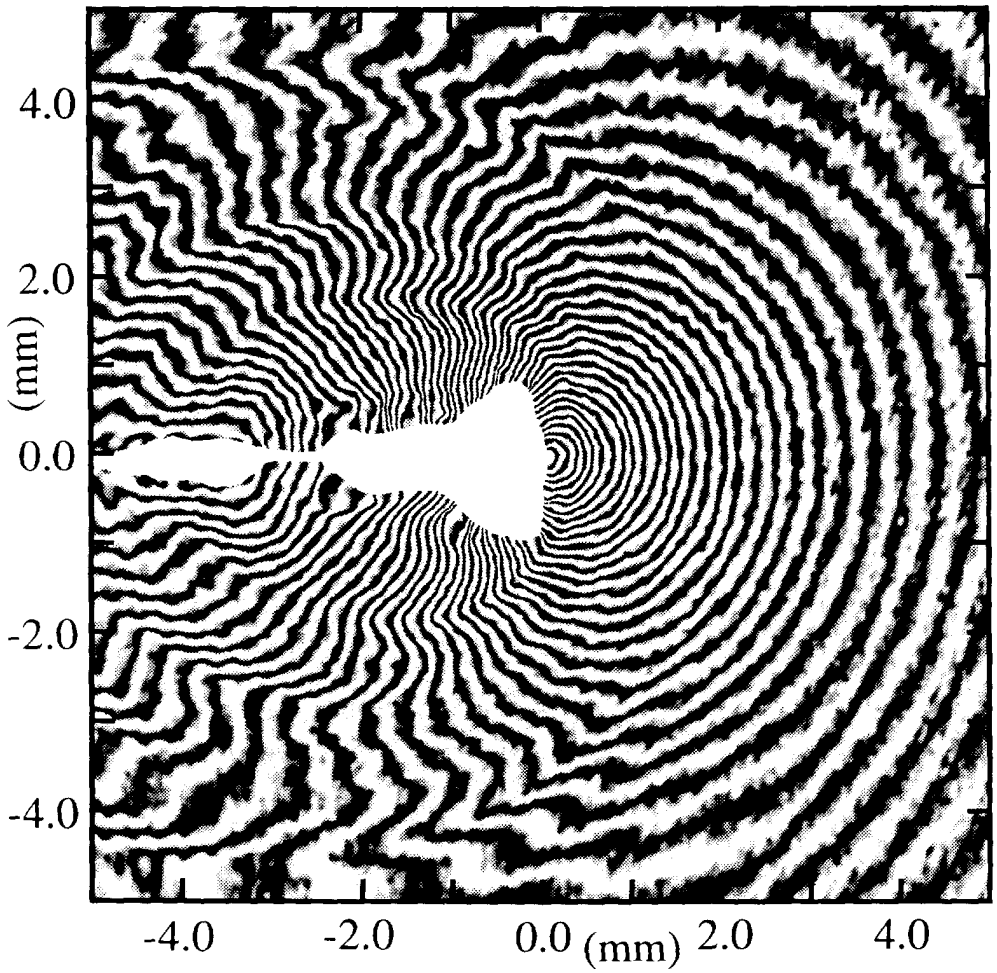

Fig. 3. A corrected interferogram (Washabaugh and Knauss, 1994) of the out-of-plane surface displacement of a crack moving at an average velocity of 0.52 mm/μs (52% of C_r) in a 4.6 mm thick virgin plate of polymethylmethacrylate. Contours represent a 257 nm change in elevation.

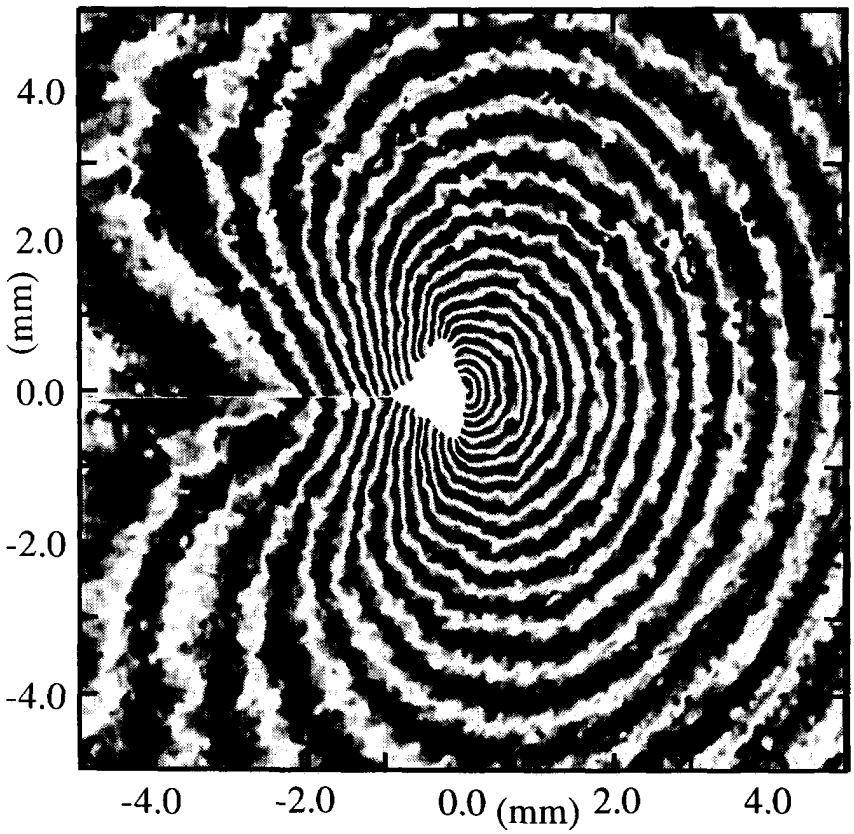

Fig. 4. A corrected interferogram (Washabaugh and Knauss, 1994) of the out-of-plane surface displacement of a crack moving at an average velocity of 0.86 mm/μs (85% of C_s) in a 4.7 mm thick interfacial plate of polymethylmethacrylate. The crack is propagating along an imperfectly sintered interface that is 60% of the strength of the virgin material. Contours represent a 257 nm change in elevation.

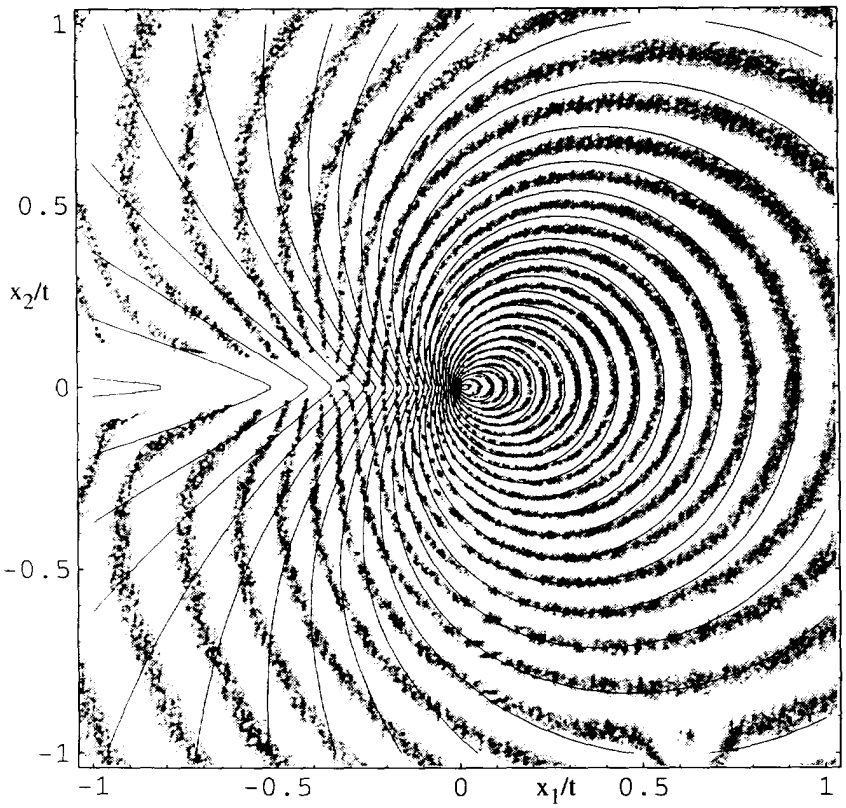

Fig. 7. Comparison of eqn (7) overlaid on the experimental data of Fig. 2.

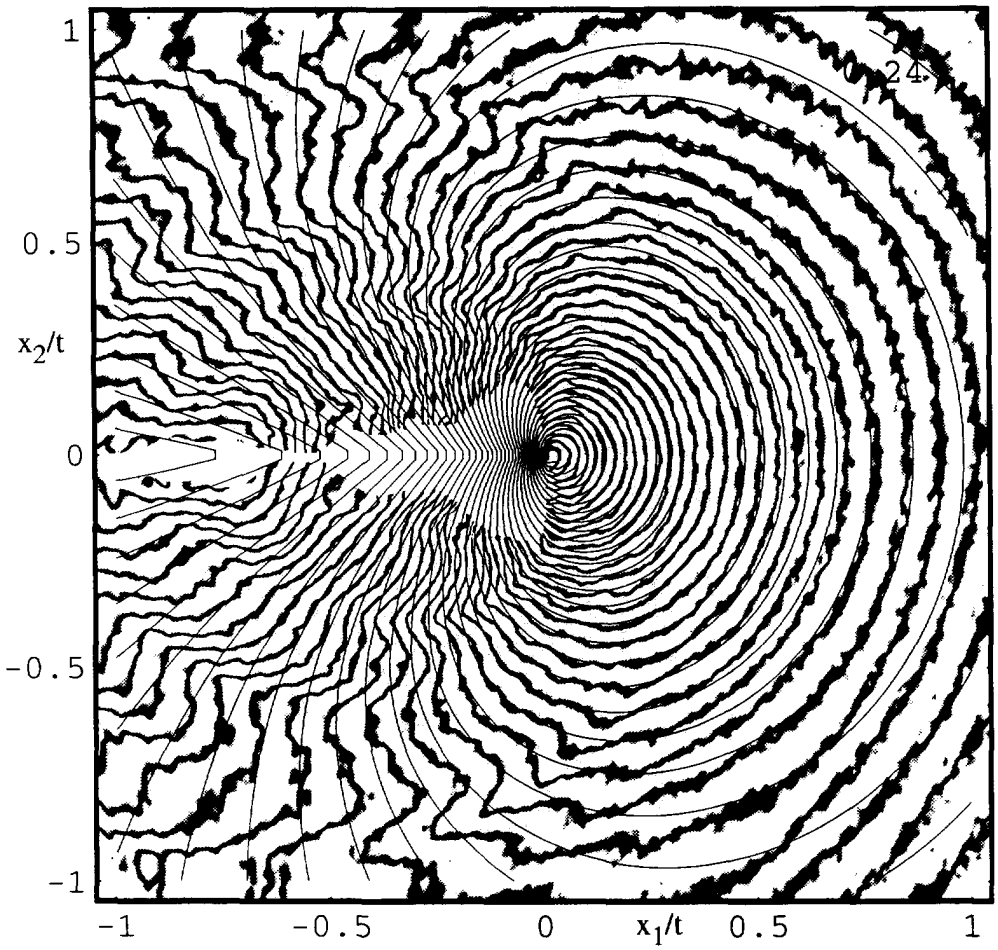

Fig. 10. A corrected interferogram of the out-of-plane surface displacement of a crack moving at an average velocity of 0.52 mm/μs in a virgin 4.6 mm thick plate of polymethylmethacrylate. Contours represent a 257 nm change in elevation.

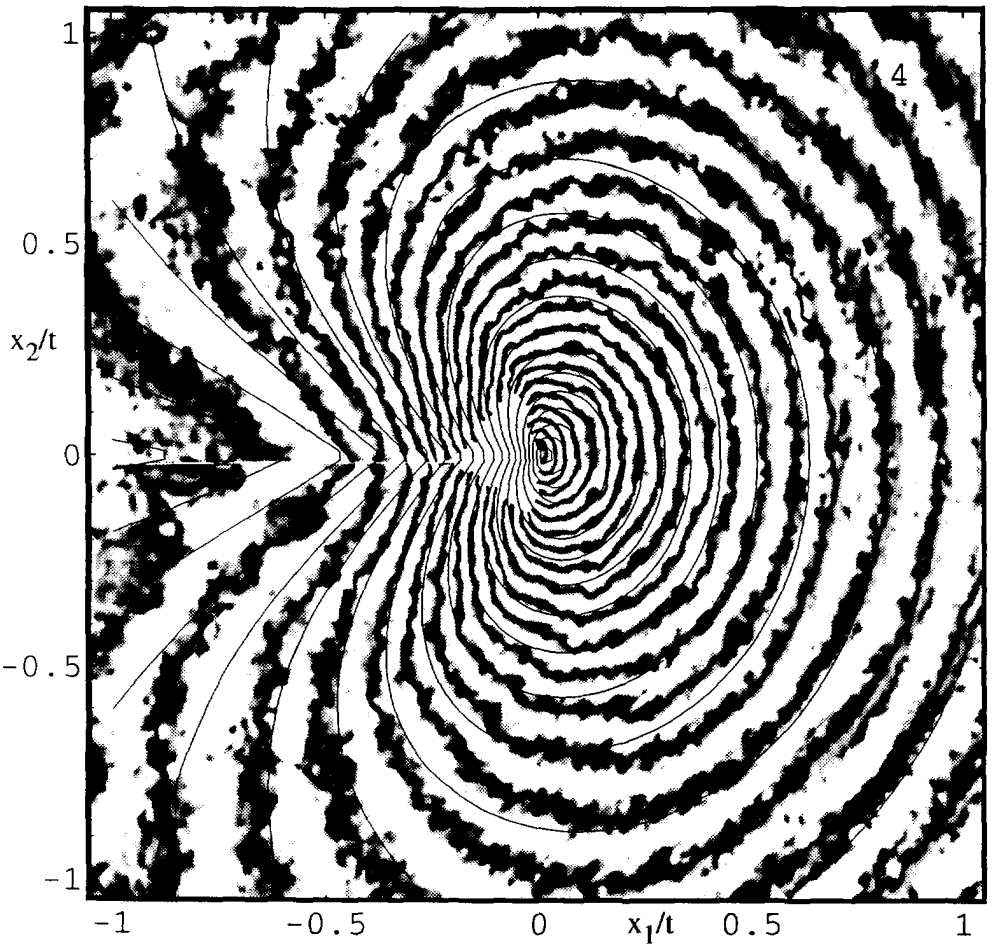

Fig. 11. A corrected interferogram of the out-of-plane surface displacement of a crack moving at an average velocity of 0.86 mm/μs in an interfacial 4.7 mm thick plate of polymethylmethacrylate. The crack is propagating along an imperfectly sintered interface that possesses 60% of the strength of the virgin material. Contours represent a 257 nm change in elevation.

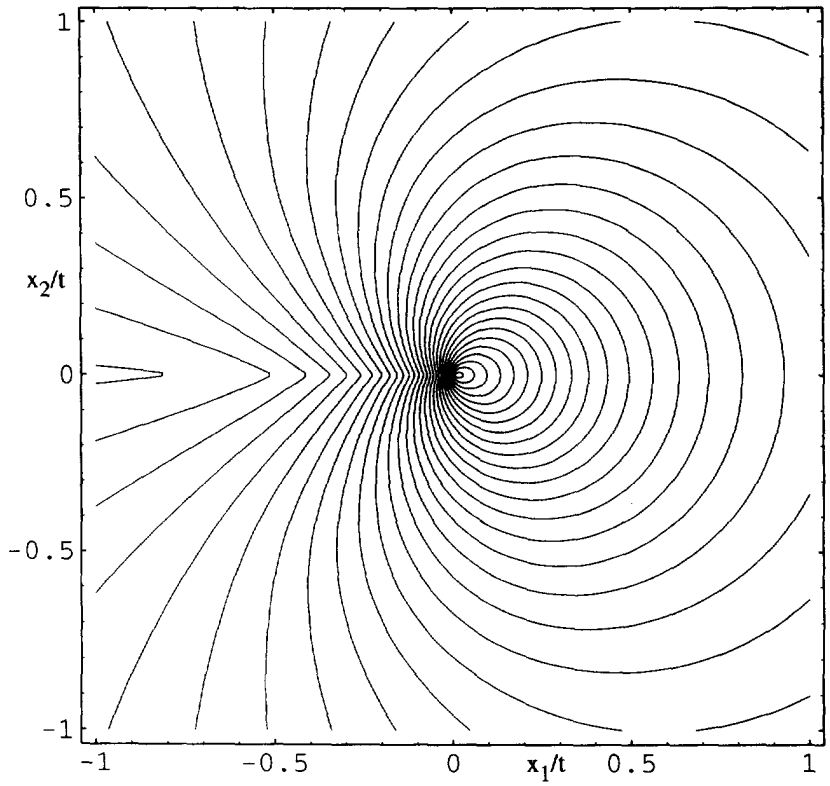

Fig. 5. Displacement contours as described from eqn (1) with the parameters given in eqn (4). This is essentially the out-of-plane displacement field predicted by Nakamura (1988).

function $\hat{u}_3^{\text{tpb}}(r_n, \theta)$ can be obtained from the original function as described by eqn (5) with the parameter b_1 found from the slope of Fig. 9(a) in Krishnaswamy *et al.* (1991):

$$\hat{u}_3^{\text{tpb}}(r_n, \theta) = \hat{u}_3(r_n, \theta) + b_1 r_n \cos\left(\frac{\theta}{2}\right) \tag{5}$$

$$b_1 = -0.035. \tag{6}$$

A plot of eqn (5), overlaid on the two- and three-dimensional results of Krishnaswamy *et al.* (1991), is shown in Fig. 6. The contours' shapes essentially match. The fact that the out-of-plane displacement gradient field from a static analysis can be used to find the gradients from a "dynamic" study foreshadows some of the discussion in the subsequent section. For this specific case, the correspondence between the out-of-plane static field and the "dynamic" field suggests that at least in terms of the out-of-plane displacement, the three point bend experiments (Krishnaswamy *et al.*, 1991) are essentially "quasi-static". Further, one might note that the addition of the higher order term is critical for this match. Ignoring this term would create a very obvious discrepancy in the shapes of the contours.

The relationship between the non-dimensional out-of-plane displacement of eqn (1) and the true displacements is shown in eqn (7):

$$u_3(r_n, \theta) = -\frac{\nu K_1 \sqrt{t}}{E} \hat{u}_3(r_n, \theta). \tag{7}$$

This result can be compared directly with the experimental measurements of the out-of-plane displacement field. In particular for, quasi-statically loaded PMMA with a Young's modulus $E = 3.1$ GPa (Washabaugh, 1990), Poisson's ratio $\nu = 0.351$ (McCammond and Motycka, 1974) and stress intensity factor $K_1 = 1.15$ MPa $\sqrt{\text{m}}$ (Washabaugh, 1990), the

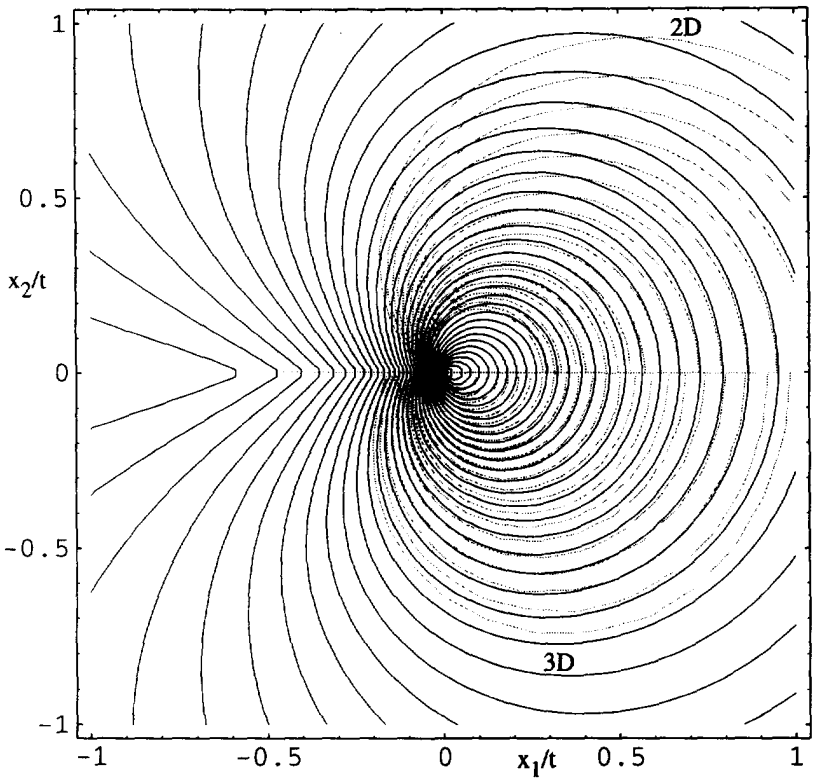

Fig. 6. Comparison of eqn (5) and Fig. 9 (c) of Krishnaswamy *et al.* (1991) for a dynamically loaded three point bend specimen.

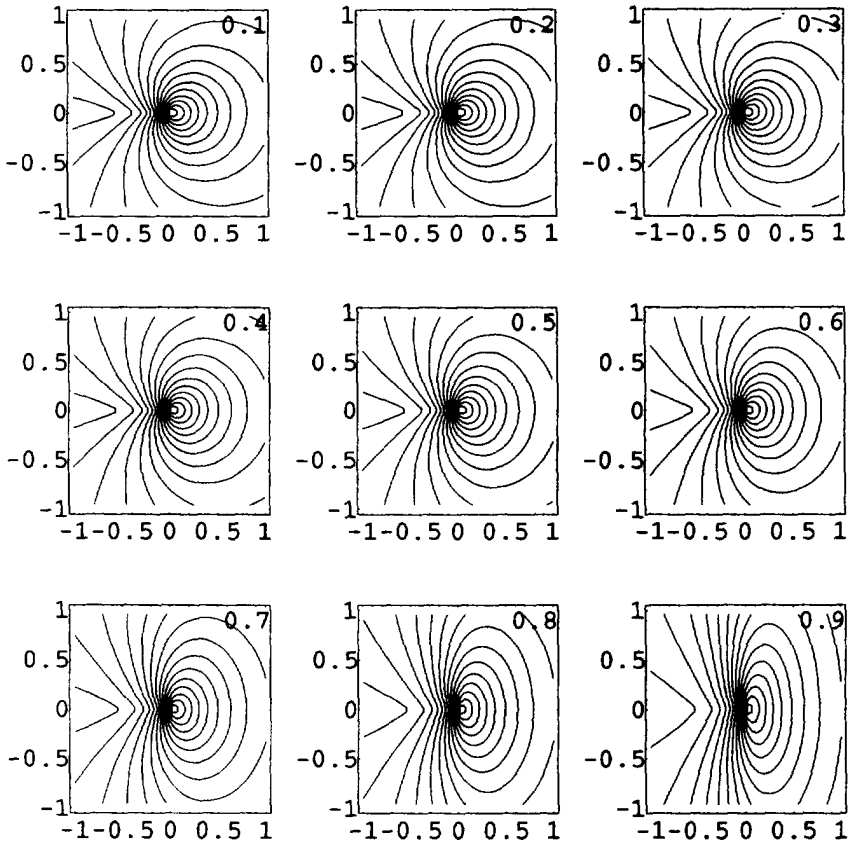

Fig. 8. Prandtl–Glauert mapping as a function of crack speed $\hat{u}_3^c\,(X_1^p(x_1,x_2), X_2^p(x_1,x_2))$ at speed ratios from 0.1 to 0.9.

theoretical surface deformation can be compared to the quasi-statically growing crack of Fig. 2. A plot of eqn (7) overlaid on a lower contrast version of the experimental data is shown in Fig. 7.

For the region in front of the slowly moving crack there is generally good agreement, between the magnitude of the slopes of the theoretical and measured displacements especially close to the crack tip. However, the shapes of the contours in front of the crack are slightly off by approximately one fringe. This discrepancy is partially due to higher order terms or may be influenced by the behavior of the material in the wake of the crack. Behind the crack, the agreement between the theoretical and measured displacements breaks down. A possible explanation which requires further study is that the theoretical crack is purely elastic, while the measured crack is slowly propagating. In other words, the displacement field presented in Fig. 2 is truly a crack and not merely an elastic notch. A hypothesis is that the discrepancy between the experimental data and theory is due at least partially to a wake of plastically deformed material. Thus the magnitude of the slope of deformation in front of a true quasi-statically propagating crack is well represented by a three-dimensional analysis. However, starting at approximately 45° to the crack flanks, there is a substantial discrepancy with the elastic analysis.

4. EFFECT OF DYNAMIC CRACK MOTION

An early study that examined aspects of the out-of-plane displacement field found that a dynamically moving crack allowed better agreement between measurement and the elastic theory along the crack flanks than a quasi-statically moving crack (Washabaugh, 1990). This is evident in Figs 3 and 4 when compared with Fig. 2. The fringes in the dynamic experiments bend back toward the crack tip in a fashion similar to Fig. 5. Thus the dynamic data, at least in terms of qualitative features along the crack flank, are actually better than the quasi-static data, perhaps because the material is fracturing in a more brittle fashion. This correspondence between the theoretical result and the dynamic data is explored further below where the objective is to examine whether a similarity transformation (Liepmann and Roshko, 1957) exists between the elastostatic deformations and those observed for steadily propagating cracks.

4.1. *Similarity rules*

Within the framework of elastodynamics, similarity transformations are used to map steady-state problems to an equivalent static problem. For example, the Prandtl–Glauert similarity transformation is used to solve steady-state problems in anti-plane shear (Freund, 1990). The general two-dimensional elastostatic plane problem is often formulated using two potentials, an in-plane dilatation potential and a two-dimensional shear potential. Likewise, the two-dimensional elastodynamic plane problem is usually formulated in terms of a dilatational potential and a shear potential. Thus, for steady-state plane dynamic problems, there holds a very simple relationship between the static and dynamic fields, wherein a separate Prandtl–Glauert transformation is applied to each of the two potentials. Further, the out-of-plane deformation associated with either the elastostatic or elastodynamic generalized plane stress is a function of the two-dimensional dilatational potential only, and therefore may be mapped directly using a single Prandtl–Glauert transformation. The fully three-dimensional steady-state elastodynamic problem involving the presence of planar traction free boundaries is considerably more complex in its relation to the elastostatic problem. It is not to be expected that the out-of-plane surface displacement field for the three-dimensional elastostatic problem may be mapped directly by a Prandtl–Glauert transformation into the out-of-plane displacement field for the equivalent steady-state elastodynamic problem. Thus, similarity between Fig. 5 and Figs 3 and 4 is investigated with the knowledge that a full accounting may not currently be possible.

4.1.1. *Prandtl–Glauert.* Since the Prandtl–Glauert mapping has been used often in the solution of steady-state continuum mechanics problems, its properties were investigated. Shown below in eqns (8) and (9) is the Prandtl–Glauert mapping between the components

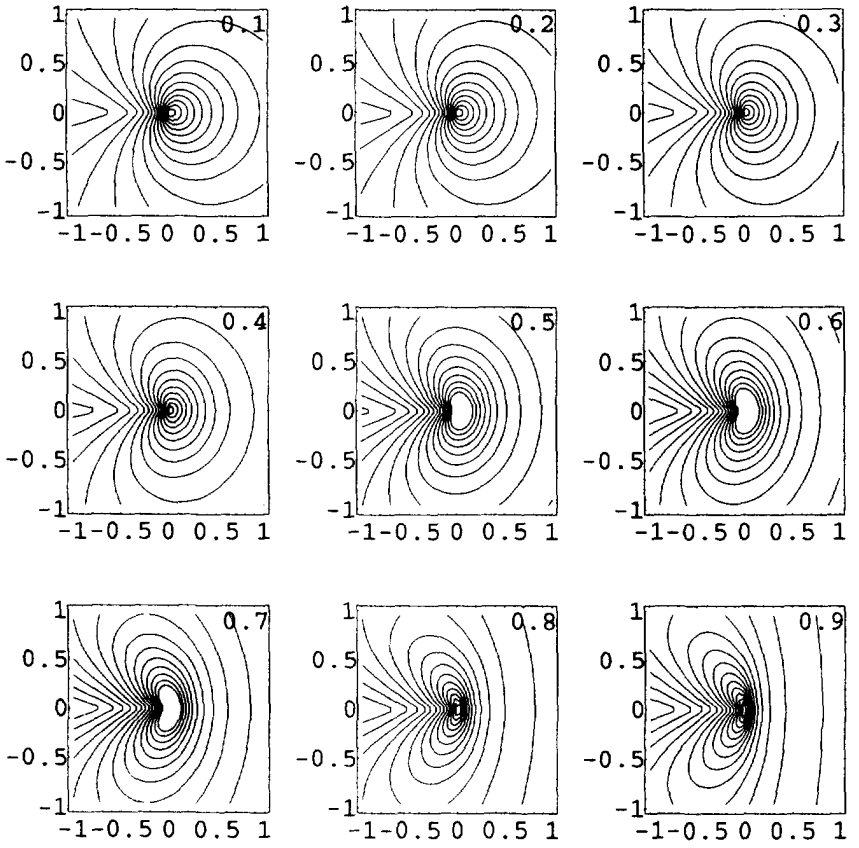

Fig. 9. Doppler mapping as a function of crack speed $\hat{u}_3^c [X_1^d(x_1, x_2), X_2^d(x_1, x_2)]$ at speed ratios from 0.1 to 0.9.

of one Cartesian frame x and another X. Here v is the steady-state crack propagation speed and c is the material wave speed. For current purposes assigning the material wave speed to either the dilatational or shear speeds is left ambiguous. In addition since this mapping deals with Cartesian components it is notationally useful to re-define the normalized out-of-plane displacement function as in eqn (10):

$$\alpha = \sqrt{1 - \left(\frac{v}{c}\right)^2} \tag{8}$$

$$X_1^p(x_1, x_2) = x_1$$

$$X_2^p(x_1, x_2) = \alpha x_2 \tag{9}$$

$$\hat{u}_3^c(x_1, x_2) = \hat{u}_3\left[\sqrt{2\pi(x_1^2 + x_2^2)}, \operatorname{atan}\left(\frac{x_2}{x_1}\right)\right]. \tag{10}$$

A series of Prandtl–Glauert mappings of the normalized out-of-plane displacement function $\hat{u}_3^c$ at speed ratios v/c between 0.1 and 0.9 is shown in Fig. 8. This mapping is of course symmetric with respect to both the ordinate and abscissa. The qualitative effect is to compress the fringe shapes in the horizontal direction. If the mappings from Fig. 8 are overlaid on Figs 3 and 4, the overall agreement is not good for any velocity ratio. However, very close to the tip elongation of the first few fringes have qualitatively the correct shape to match the fringes at the tips of both interferograms if they are scaled by the shear wave speed. In other words, the shape of the fringes at the tip of the crack is compressed by an amount consistent with a Prandtl–Glauert mapping when c is equal to the shear wave

speed. For Figs 3 and 4, this corresponds to a crack speed ratio of 0.5 and 0.8, respectively. This is not a very strong statement since only one fringe is being compared and the ability of these tests to discern fringe shapes is diminished at the crack tip due to the small amount of data collected near the tip.

4.1.2. *Doppler.* A second mapping can be explored by considering the difference in the motion of waves radiating from a stationary versus a steadily moving source. This is called a Doppler mapping which takes originally concentric circles and transforms them to non-concentric circles. The centers of the transformed circles are equally spaced along the propagation path of the source (Liepmann and Roshko, 1957). An explicit form of this mapping is shown in eqn (11). The inverse of this mapping is typically more recognizable and is given in eqn (12):

$$X_1^{\mathrm{d}}(x_1, x_2) = x_1 + \frac{v}{c}\left(\frac{\frac{v}{c}x_1 + \sqrt{x_1^2 + \alpha^2 x_2^2}}{\alpha^2}\right) \tag{11}$$

$$\begin{aligned} X_2^{\mathrm{d}}(x_1, x_2) &= x_2 \\ x_1^{\mathrm{d}}(X_1, X_2) &= X_1 + \frac{v}{c}\sqrt{X_1^2 + X_2^2} \\ x_2^{\mathrm{d}}(X_1, X_2) &= X_2. \end{aligned} \tag{12}$$

A series of Doppler mappings of the normalized out-of-plane displacement function $\hat{u}_3^c$ at speed ratios v/c between 0.1 and 0.9 is shown in Fig. 9. This mapping is symmetric with respect to the abscissa. The qualitative effect is to shift the fringes by varying degrees with respect to radial distance in the negative horizontal direction. More importantly the mapping develops lobes in the fringe pattern that are also evident in the experimental data.

4.2. *Comparison with dynamic experimental data*

If the material wave speed c is set to the dilatational wave speed and specific contours are generated for the two dynamic interferograms, the general fit of the Doppler transformation can be ascertained. Shown in Figs 10 and 11 are the specific mapped contours for each of the dynamic interferograms overlaid on a reduced contrast version of the images of Figs 3 and 4, respectively. Note that the non-dimensional out-of-plane displacements are compared with the interferograms. Thus, only the contour shapes and relative spacing are being compared. This is partially justified since both the propagation stress intensity and the modulus under dynamic conditions increase in approximately the same proportion (Washabaugh, 1990).

For both sets of data the mapped theoretical shapes within a normalized radius of 0.5 agree quite well. At larger radial distances, asymmetries are evident in the data and the agreement is less impressive. Perhaps the most significant discrepancy is the difference in fringe spacing at the large radial distances. Clearly a simple Doppler mapping does not account for some aspect of the magnitude of the deformation. Perhaps these are due to some higher order effects [for example Taudou *et al.* (1992)].

One other easily recognizable difficulty is the phenomenon of waves radiating from the crack tip and causing the fringes to exhibit wiggles. The latter have not been accounted for in this analysis. Thus, the gross features of the out-of-plane displacement of a steadily propagating crack can be accounted for by a dilatational wave scaled Doppler mapping of the static three-dimensional field. A shear wave scaling or a Prandtl–Glauert mapping does not work.

5. SUMMARY AND DISCUSSION

The theoretical out-of-plane displacement function representing the corresponding static problem appears to predict the surface slopes preceding a quasi-statically propagating crack. The reason for the discrepancy in the wake of the crack requires further investigation but is potentially due to plasticity or viscoelasticity of the material. One could easily imagine using this approach to effectively calculate K_I as long as only the data in front of the crack is used, and the crack behaves in a sufficiently brittle manner. Thus, in an existing structure, it may be practical to make an *in situ* non-destructive measurement of the plane–normal surface deformation near the tip of an existing (and properly configured) crack to determine its current stress intensity.

In addition, gross features of the dynamic interferograms near the crack tip are better described by a Doppler similarity transformation of the elastostatic solution than by a Prandtl–Glauert mapping. This transformation is successful, provided the wave speed used in the mapping is taken as the dilatational wave speed. Further study is required, perhaps with an elastodynamic simulation, to truly account for the data. It is important to note here that the out-of-plane displacement field for a rapidly propagating crack is significantly different than the elastostatic field. Thus, experimental techniques which incorporate measurement of the out-of-plane displacement and rely on calibration using a static crack need significant adjustment when used in a dynamic scenario.

REFERENCES

Bradley, W. B. and Kobayashi, A. S. (1970). An investigation of propagating cracks by dynamics photoelasticity. *Expl Mech.* **10,** 106–113.

Burton, W. S., Sinclair, G. B., Solecki, J. S. and Swedlow, J. L. (1984). On the implications for LEFM of the three-dimensional aspects in some crack/surface intersection problems. *Int. J. Fract.* **25,** 3–32.

Creath, K. (1989). Calibration of numerical aperture effects in interferometric microscope objectives. *Appl. Optics* **28,** (15), 333.

Dudderar, T. D. and O'Regan, R. (1971). Measurement of the strain field near a crack-tip in polymethylmethacrylate by holographic interferometry. *Expl Mech.* **11,** 49–56.

Freund, L. B. (1990). *Dynamic Fracture Mechanics.* Cambridge University Press, Cambridge.

Griffith, A. A. (1920). The phenomenon of rupture and flow in solids. *Phil. Trans. R. Soc. London* **A221,** 163–198.

Irwin, G. R., Dally, J. W., Kobayashi, T., Fourney, W. L., Etheridge, M. J. and Rossmanith, H. P. (1979). On the determination of the a–K relationship for birefringent polymers. *Expl Mech.* **19,** 121–128.

Kim, K. S. (1985). A stress intensity factor tracer. *ASME J. Appl. Mech.* **52,** 291–297.

Knauss, W. G. and Ravi-Chandar, K. (1985). Some basic problems in stress wave dominated fracture. *Int. J. Fract.* **27,** 127–143.

Krishnaswamy, S., Rosakis, A. J. and Ravichandran, G. (1991). On the extent of dominance of asymptotic elastodynamics crack-tip fields. Part II—Numerical investigation of three-dimensional and transient effects. *J. Appl. Mech.* **58,** 95–103.

Liepmann, H. W. and Roshko, A. (1957). *Elements of Gasdynamics.* Wiley, New York.

McCammond, D. and Motycka, J. (1974). Strain-ratio measurements by an interferometric device. *Expl Mech.* **14,** 225–229.

Nakamura, T. and Parks, D. M. (1988). Three-dimensional field near the crack front of a thin elastic plate. *J. Appl. Mech.* **55**(4), 805–813.

Parsons, I. D., Hall, J. F. and Rosakis, A. J. (1986). A finite element investigation of the elastostatic state near a three-dimensional edge crack. GALCIT SM Report 86-29, California Institute of Technology, Pasadena, CA.

Pfaff, R. D. (1991). Three-dimensional effects in nonlinear fracture explored with interferometry. Ph.D. thesis, Graduate Aeronautical Laboratories, California Institute of Technology, Pasadena, CA.

Pfaff, R. D., Schultheisz, C. R. and Knauss, W. G. (1994). An experimental/analytical comparison of 3-D deformation at the tip of a crack in a plastically deforming plate. Part I: optical interferometry and experimental preliminaries (in preparation).

Rosakis, A. J. and Zehnder, A. T. (1985). On the method of caustics: an exact analysis based on geometrical optics. *J. Elasticity* **15,** 374–367.

Smith, C. W. (1973). Use of 3D photoelasticity in fracture mechanics. *Expl Mech.* **13,** 539–544.

Smith, R. H. and Freund L. B. (1988). Three-dimensional finite element analysis of steady elastodynamic crack growth in a plate. ASME-SES Conf. Berkeley, CA.

Sokolnikoff, I. S. (1956). *Mathematical Theory of Elasticity.* Kreiger Publishing, Malabar, FL.

Sutton, M. A., Turner, J. L., Chao, Y. J., Bruck, H. A. and Chae, T. L. (1992). Experimental investigations of three-dimensional effects near a crack tip using computer vision. *Int. J. Fract.* **53,** 201–228.

Taudou, C., Potti, S. V. and Ravi-Chandar, K. (1992). On the dominance of the singular dynamic crack tip stress field under high rate loading. *Int. J. Fract.* **56,** 41–59.

Theocaris, P. S. (1963). Diffused light interferometry for measurements of isopachics. *J. Mech. Phys. Solids* **11,** 181–195.

Tippur, H. V., Krishnaswamy, S. and Rosakis, A. J. (1991). Optical mapping of crack tip deformations using the methods of transmission and reflection coherent gradient sensing: as study of crack tip *K*-dominance. *Int. J. Fract.* **52,** 91–117.

Washabaugh, P. D. (1990). An experimental investigation of mode-I crack tip deformation. Ph.D. thesis, California Institute of Technology, Pasadena, CA.

Washabaugh, P. D. and Knauss, W. G. (1993). Non-steady, periodic behavior in the dynamic fracture of PMMA. *Int. J. Fract.* **59,** 189–197.

Washabaugh, P. D. and Knauss, W. G. (1994). A reconciliation of dynamic crack velocity and Rayleigh wave speed in isotropic brittle solids. *Int. J. Fract.* **65,** 97–114.

Wells, A. and Post, D. (1954). The dynamic stress distribution surrounding a running crack—a photoelastic analysis. *Proc. SESA* **XVI,** 69–92.

Williams, M. L. (1957). On the stress distribution at the base of stationary crack. *J. Appl. Mech.* **24,** 109–144.